EasyChair Preprint

№ 15233

Wheat Fusarium Head Blight Disease Severity Estimation Using UAS Multispectral Imagery and Machine Learning

Ubaid Ur Rehman Janjua, Maitiniyazi Maimaitijiang,
Bruce Millett, Dalitso Yabwalo, Kamila Dilmurat,
Shahid Nawaz Khan, Mohammad Maruf Billah, Madalyn Shires,
Sunish K. Sehgal and Shaukat Ali

October 18, 2024

Wheat Fusarium Head Blight Disease Severity Estimation using UAS Multispectral Imagery and Machine Learning

Ubaid ur Rehman Janjua[1], Maitiniyazi Maimaitijiang[1] , Bruce Millett[1*] , Dalitso Yabwalo[2] , Kamila Dilmurat[3] , Shahid Nawaz Khan[4], Mohammad Maruf Billah[1] , Madalyn Shires[2] , Sunish K. Sehgal[2], Shaukat Ali[2]*

[1]Department of Geography and Geospatial Sciences, Geospatial Sciences Center of Excellence, South Dakota State University, Brookings, SD 57007, USA

[2]Department of Agronomy, Horticulture, and Plant Science, South Dakota State University, Brookings, SD 57007, USA

[3]Department of Civil and Environmental Engineering, University of California Merced, Merced 95343, USA

[4]Department of Geography and the Environment, University of Alabama, Tuscaloosa 35401, USA

***Abstract*—Wheat is an important primary crop that feeds billions of people worldwide. Wheat diseases, particularly Fusarium Head Blight (FHB) disease often have severe effects on wheat yield quantity and quality, and also potentially threaten the health of humans and livestock. Traditional field surveying-based methods for monitoring and assessment of wheat diseases are time-consuming and inefficient. Remote sensing approach, particularly aerial imaging using Uncrewed Aircraft Systems (UAS) has become an essential tool for fine-scale and rapid field scouting and crop disease monitoring in recent years. The work is to investigate the potential of combination of high-resolution UAS multispectral imagery with machine learning (ML) methods in detection of FHB disease severity. Two experimental wheat fields are setup in Brookings, South Dakota, USA in 2022. The severity of FHB disease was assessed periodically through visual observation; and synchronous UAS flights were conducted to collect multispectral imagery. UAS multispectral imagery-based canopy spectral and texture features were derived, and used as input variables to develop ML-based classification and regression models for FHB disease severity estimations. Conventional ML methods such as Support Vector Machine (SVM), Random Forest (RF), along with deep learning models, Deep Neural Network (DNN), and One-Dimensional Convolutional Neural Network (1D-CNN) were employed. The results show that both canopy spectral and texture features are important variables for wheat FHB disease severity estimations. Additionally, UAS remote sensing, coupled with ML-based classification and regression approaches is a viable approach to rapidly and accurately estimate and assess wheat FHB disease severity at a fine-scale for large areas.**

Keywords—Uncrewed Aircraft Systems (UAS); Fusarium Head Blight (FHB); spectral features; texture features; machine learning

I. INTRODUCTION

Wheat is the third most cultivated grain crop globally after rice and corn, and it ranks third in the United States after corn and soybeans in terms of planted acreage, production, and gross farm revenues [1]. Wheat production safety is important for global food security, economic stability, and effective planning for future crop strategies [2]. Various diseases caused by bacteria and fungi can significantly affect wheat grain yield and quality. Among these, Fusarium head blight (FHB), an intrinsic infection caused by Fusarium graminearum (Gibberella zeae), has become a globally significant fungal disease that poses a major threat to the growth of wheat [3]. FHB infected wheat crops can produce mycotoxins such as deoxynivalenol (DON) and zearalenone (ZEA), which may persist in wheat spikes. These mycotoxins pose significant threats to human and livestock health, potentially leading to acute poisoning symptoms, the destruction of immunity, and even death. Ultimately, FHB can lead to reduced grain yield and quality loss, lower fungicide costs, and increased profitability [4, 5].

Therefore, rapid and precise monitoring and mapping of wheat FHB disease severity is essential for farmers to identify infected areas within sub-field level, enabling timely management and decision-making; and it is also beneficial in terms of plant phenotyping [4]. Traditional method of FHB disease scouting and monitoring is often through field visits and visual observations. This approach is often time-consuming, costly, and inefficient especially when large areas are monitored [6].

In recent years, the rapid development of low-altitude aerial imaging and remote sensing, particularly Uncrewed Aircraft Systems (UAS) platforms and sensor technologies, has enabled the acquisition of high-resolution RGB, multispectral, hyperspectral, LiDAR, and thermal data [7]. UAS remote sensing has been widely used for fine-scale crop growth monitoring, disease detection and mapping [8], different plat traits estimation [9], grain yield and quality estimation [10].

In terms of aerial imaging and UAS remote sensing-based wheat diseases such as FHB severity estimation, the previous studies mainly employed ML-based classification approach [8, 11], and regression modeling approach is less explored. Additionally, spectral features derived from UAS RGB [12], multispectral [13], or hyperspectral [8] imagery were utilized as input variables for crop disease severity estimation model, the potential of UAS imagery-based texture features, as well as spectral and texture feature fusion is less attempt for crop disease severity estimations [14, 15]. Particularly in the case of wheat FHB disease severity prediction [16]. Therefore, this study investigates the potential of high-resolution UAS multispectral image-derived spectral and textural features, along with their

combinations, for identifying and estimating wheat FHB disease severity using both conventional ML, and deep learning-based classification and regression approaches

II. Test Sites And Data

A. Test sites and experimental setup

Wheat experimental fields were established at a research farm of South Dakota State University located at Brookings, South Dakota (Figure 1). Wheat FHB spray inoculation was carried out during the spring 2022. The test site experiences a humid continental climate [17], and characterized by typically warm summers and freezing, snowy, and windy winters. Throughout the year, temperatures generally range from -13.00°C to 28.33°C and rarely fall below -25.00°C or exceed 33.33°C. The mean annual precipitation at this site is approximately 559 millimeters. The soils are moderately well-drained and formed in loess overlying glacial till on foot slopes and in swales.

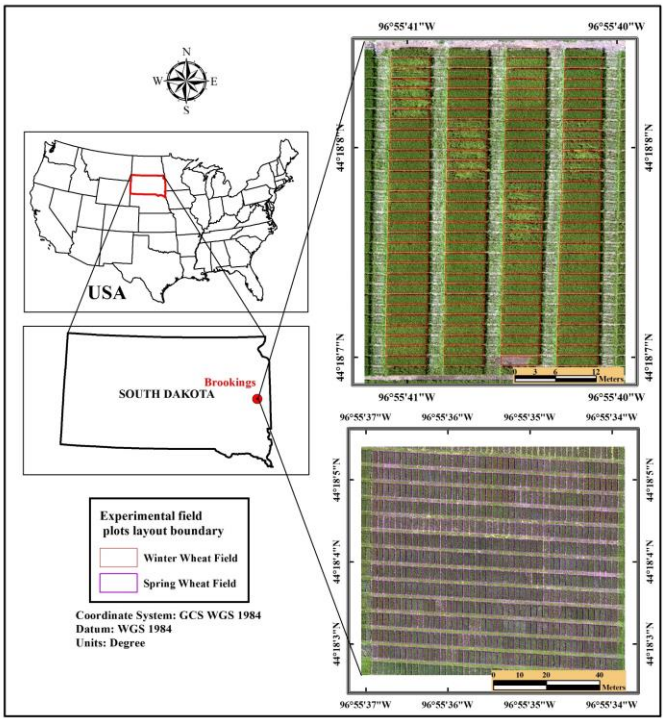

Fig. 1. Test site location and field layout map

B. Data collection and preprocessing

Periodical field surveying and disease severity rating were conducted during June and July of 2022, and the specific severity percentage of FHB diseases at each plot was recorded. A total of 119 FHB disease severity data samples from the winter wheat field and 240 samples from the spring wheat field were collected (Figure 1).

UAS campaigns were synchronized with field surveying to collect high-resolution multispectral imagery. A DJI Matrice 300 RTK (Figure 2 (A)) UAS platform integrated with a Micasense Altum multispectral camera (Figure 2 (B)) was used to collect multispectral data. The Altum multispectral camera features blue, green, red, red-edge, and near-infrared (NIR) bands (Fig. 2 (B)) with a 3.2MP sensor resolution and is integrated with a real-time downwelling light sensor.

The UAS flight was conducted at an altitude of 50 meters and a flight speed of 5 m/s, with 80% side and frontal overlaps. Agisoft Metashape software was used for UAS imagery ortho-mosaicking and radiometric calibration, while ArcGIS software was employed to create plot boundaries, which were further used to derive plot-level image features.

Fig. 2. The UAS platform (A) and Altum multispectral sensor (B) used in this work; photos of wheat FHB disease infected wheat canopy.

The field survey-based wheat FHB disease severity data (the unit is a percentage) was categorized into five disease levels as shown in Table 1, which is used for ML-based FHB disease severity level classification modeling.

TABLE I. FHB DISEASE SEVERITY (%) CATEGORIES

Class	Severity% range	Severity level	No. of Samples
1	0-10%	Very low	98
2	<10-20%	Low	110
3	<20-30%	Moderate	71
4	<30-40%	High	29
5	<40%	Very high	51

III. Methods

A. Image feature extraction

A variety of spectral features such as vegetation indices [18] were derived, and plot level mean values of each spectral feature were calculated and used as input variables for ML-based wheat FHB disease severity estimations [19].

In addition to spectral features, the grey level co-occurrence matrix (GLCM) canopy texture features were also derived from the UAS multispectral imagery. GLCM, introduced by [20], is a widely used image texture feature in remote sensing applications. It characterizes the joint probability of pixel pairs at any grey level and statistically represents an image's texture. Eight GLCM-based features, namely mean (M.E.), variance (V.A.), homogeneity (H.O.), contrast (C.O.), dissimilarity (DI), entropy (EN), second moment (S.M.), and correlation (CC) were

calculated and used as input variables for ML-based wheat FHB diseases severity estimations.

B. Modeling methods

UAS multispectral imagery-derived plot-level mean spectral and texture features were used as input variables for ML-based classification and regression models. Conventional ML algorithms, including Support Vector Machine (SVM) and Random Forest (RF), along with deep learning methods such as Deep Neural Networks (DNN), and One-Dimensional Convolutional Neural Network (1D-CNN) were used to predict FHB disease severity. The performance of ML-based classification and regression models were investigated using spectral, textural features, along with their combinations as input variables in wheat FHB disease severity estimations, respectively.

C. Model development and assessment

70% of randomly selected wheat FHB disease data points were used as training data, and the remaining 30% of samples were used for model testing. Hyperparameter tuning was conducted for all ML models to derive optimal modeling results. The overall diagrammatic workflow, including UAS image processing, model development, and assessment, is presented in Figure 3. For the classification method, overall accuracy (Eq. 1), kappa coefficient (Eq. 2), and f-score (Eq. 3) were used as evaluation metrics.

$$\text{Overall Accuracy} = \frac{TP+TN}{TP+TN+FP+FN} \quad (1)$$

$$Kappa\ Coefficient = \frac{p0-pe}{1-pe} \quad (2)$$

$$f-score\ = 2 * \frac{Precision \times Recall}{Precision+Recall} \quad (3)$$

Po is the observed accuracy and *Pe* is the expected accuracy by chance, *TP* represents true positives, *TN* represents true negatives, *FP* represents false positives, and *FN* represents false negatives. Precision is calculated as *TP/TP+TP* and recall is calculated as *TP/TP + FN*.

For regression, the coefficients of determination (R^2) (Eq. 4), root mean square error (RMSE) (Eq. 5), and relative RMSE (RMSE%) (Eq. 6) were used as model evaluation metrics to assess and compare the performance of machine learning models.

$$R^2 = 1 - \frac{\sum_{i=1}^{n}(y_i-\hat{y}_i)^2}{\sum_{i=1}^{n}(y_i-\bar{y})^2} \quad (4)$$

$$RMSE = \sqrt{\frac{\sum_{i=1}^{n}(y_i-\hat{y}_i)^2}{n-1}} \quad (5)$$

$$RMSE\% = \frac{RMSE}{\bar{y}} * 100 \quad (6)$$

Where n is the number of FHB data points used during the model testing phase, $\hat{y}_i$, y_i and $\bar{y}$ corresponding to the estimated, measured and mean of the measured FHB severity values.

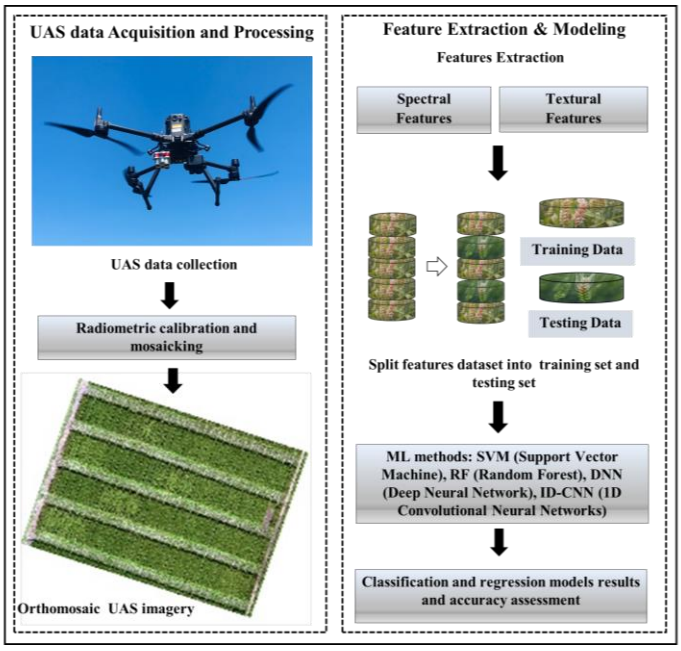

Fig. 3. Workflow diagram of UAS data collection, processing, feature extraction, ML-based modeling, and accuracy assessment

IV. Results and Discussion

A. ML-based FHB severity level classification results

UAS imagery-derived spectral, texture features and their combinations, were used as input variables, respectively, to predict FHB disease severity levels (i.e., Very low, Low, Moderate, High, and Very high five categories) using SVM, RF, DNN, and 1D-CNN based classification models. The model testing results, as shown in Table II and Figure 4, demonstrate that both spectral and texture features can effectively predict FHB severity levels, with overall accuracy ranging from 0.54 to 0.62 for spectral features and from 0.56 to 0.80 for texture features. Spectral features yielded superior results with the RF and 1D-CNN methods, while texture features demonstrated higher accuracy with the SVM and DNN methods. This suggests that both spectral and texture features are important indicators for identifying FHB disease severity [16].

The combination of spectral and texture features outperformed the use of spectral features alone, regardless of the classification model. Moreover, the fusion of spectral and texture features also demonstrated higher accuracy compared to using texture features alone in the case of the RF and 1D-CNN models. Spectral and texture features exhibit overlapping and redundant information; therefore, combining these two feature types may not consistently lead to improved model performance. This finding is consistent with previous studies [21].

In terms of the performance of ML-based classification models, the conventional machine learning method RF achieved the highest classification accuracy (0.69) when using spectral features, while the deep learning method DNN resulted in the lowest accuracy (0.54). For texture features, SVM outperformed other models with an overall accuracy of 0.80, whereas the deep learning method 1D-CNN yielded the lowest accuracy at 0.56.

The poorer performance of deep learning methods is likely due to the smaller sample size for model training [22]. It is worth noting that, in the case using combined features, 1D-CNN and RF outperformed the case of using the spectral or texture features alone, indicating the superior performance of these methods in handling high dimensional and redundant features to some extent [23].

TABLE II. VALIDATION MATRIX OF FHB DISEASE SEVERITY CLASSIFICATION RESULTS

Features	Validation matrix	SVM	RF	DNN	1D-CNN
Spectral	Overall Accuracy	0.57	0.69	0.54	0.62
	Kappa Coefficient	0.43	0.60	0.38	0.50
	f-score	0.56	0.68	0.53	0.62
Textural	Overall Accuracy	0.80	0.58	0.67	0.56
	Kappa Coefficient	0.73	0.45	0.54	0.41
	f-score	0.79	0.57	0.67	0.56
Spectral + Textural	Overall Accuracy	0.70	0.70	0.56	0.72
	Kappa Coefficient	0.62	0.61	0.40	0.63
	f-score	0.70	0.69	0.52	0.72

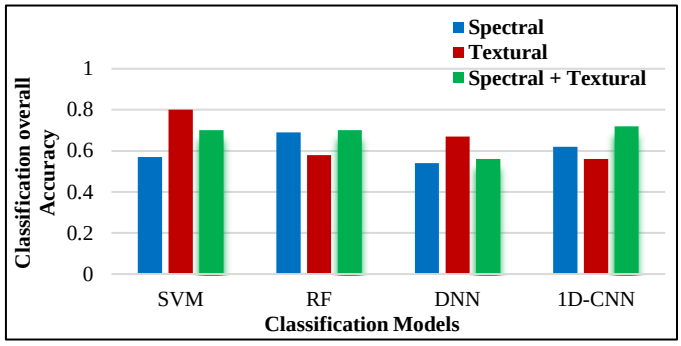

Fig. 4. FHB severity classification results comparison.

Figure 5 presents the confusion matrix of different ML models at the testing phase when using combined spectral and textural features in wheat FHB disease severity levels classification. Misclassification primarily occurs among the very low, low, and moderate categories of FHB disease severity across most ML classification models, resulting in lower classification accuracies (from 33% to 70%) for these categories. Additionally, most ML models achieved high classification accuracy (above 83%) for the high and very high FHB disease severity categories.

The results suggest that at low to moderate levels of FHB disease (Table 1 and Figure 2C), the spectral and texture signals captured by UAS imagery are similar to some extent. However, these signals showed significant differences when the wheat canopy experienced severe levels of FHB disease (i.e., High and Very high levels of FHB disease severity in our work).

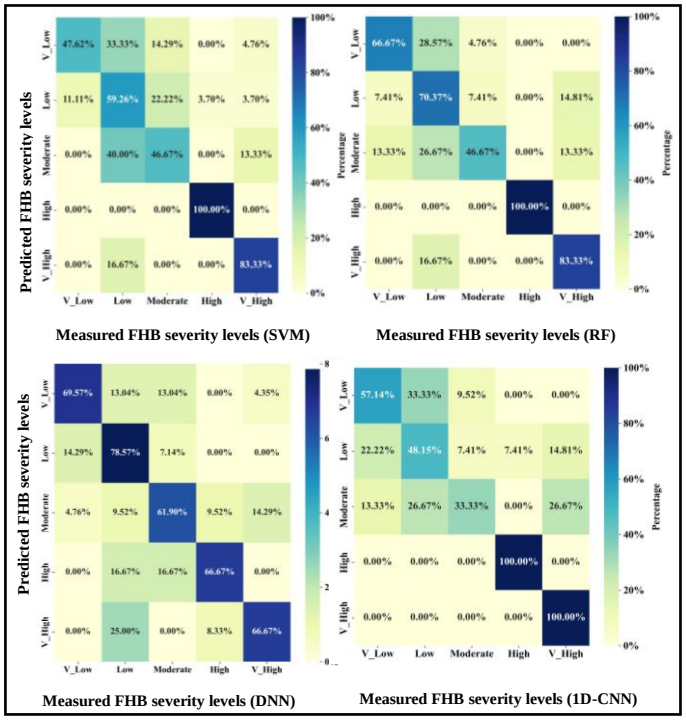

Fig. 5. Confusion matrics of FHB severity classification results from different ML models when using combined spectral and texture features.

B. ML-based regression analysis of FHB wheat disease

UAS imagery-derived spectral, texture features and their combinations, were used as input variables, respectively, to estimate FHB disease severity (express as a percentage (Table 1 and Figure 2C)) using SVM, RF, DNN, and 1D-CNN based regression models. The regression model testing results (Table III and Figure 6) illustrate that both spectral and texture features can estimate FHB severity to some extent, with R^2 ranging from 0.44 to 0.73 for spectral features, and from 0.51 to 0.63 for texture features. Spectral features yielded superior results with the SVM and RF models, while texture features demonstrated slightly higher accuracy with the DNN and 1D-CNN models. This suggests that both spectral and texture features are important indicators for estimating and assessing FHB disease severity in the context of using ML-based regression modeling [16]. The combination of spectral and texture features outperformed the use of spectral features alone in the DNN and 1D-CNN models, and outperformed texture features alone in the SVM and 1D-CNN models. However, because spectral and texture features exhibit overlapping and redundant information, combining them did not consistently improve regression model performance, as was observed in the classification models.

When comparing ML-based regression models for FHB disease severity estimation, the conventional machine learning method SVM achieved the highest estimation accuracy (R^2=0.73) using spectral features, while the deep learning method DNN produced the lowest estimation accuracy (R^2=0.44). In the case of using texture features, RF outperformed other regression models with an R^2 of 0.63, whereas the deep learning method 1D-CNN yielded the lowest accuracy with an R^2 of 0.48. In the case of using spectral and texture combined features, RF outperformed other regression

models with an R^2 of 0.63, whereas the deep learning method DNN yielded the lowest accuracy with an R^2 of 0.50. The relatively poorer performance of deep learning methods when using different features as input variables, is likely due to the smaller sample size for model training [22]. Future work could focus on further testing the potential of deep learning models by utilizing larger sample sizes, as well as employing pre-trained deep learning models through deep transfer learning approach to address the challenges associated with small sample sizes.

TABLE III. VALIDATION METRICS OF FHB SEVERITY ESTIMATION RESULTS USING REGRESSION MODELING APPROACHES

Features	Metrics	SVM	RF	DNN	1D-CNN
Spectral	R^2	0.73	0.66	0.44	0.45
	RMSE	8.56	8.88	11.6	12.3
	RMSE%	39.7	43.1	58.9	57.2
Texture	R^2	0.52	0.63	0.51	0.48
	RMSE	10.4	10.1	10.2	12.1
	RMSE%	50.8	46.2	49.1	56.6
Spectral + Textural	R^2	0.57	0.63	0.50	0.52
	RMSE	10.8	10.1	11.7	11.5
	RMSE%	49.6	48.6	53.8	52.6

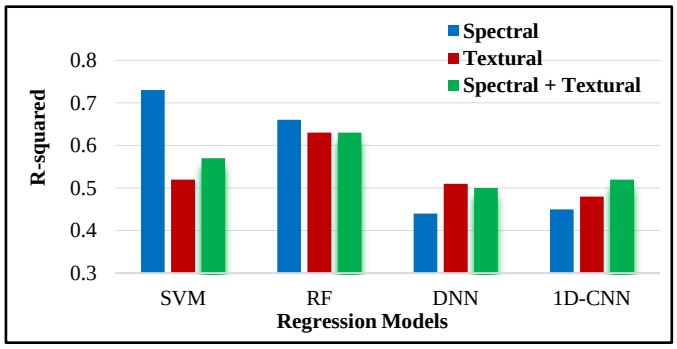

Fig. 6. Comparison of FHB severity estimation results from different regression models.

Figure 7 presents a scatter plot (also known as a 1:1 plot) that comparing the measured FHB disease severity with the predicted results from different ML-based regression models when using the combined spectral and texture features. FHB disease severity below 20% was overestimated across all ML regression models, which may have contributed to the relatively lower R^2 values (ranging from 0.50 to 0.63) observed in these models. This also highlights the challenges in accurately estimating FHB disease at lower severity levels. A certain level of underestimation was observed from all ML regression models when FHB severity ranged from 20% to 60% from the scatter plot (Figure 6). Overall, ML-based regression modeling using UAS multispectral imagery is capable of estimating wheat FHB disease severity to some extent. The relatively lower accuracy in both classification and regression approaches may be attributed to a few factors: the small size of wheat spikes, relative to the entire wheat canopy of each plot (or sampling spot) captured by the UAS multispectral camera, may not significantly influence the spectral and texture signals. Additionally, the small sample size poses challenges in training machine learning models, particularly deep learning models.

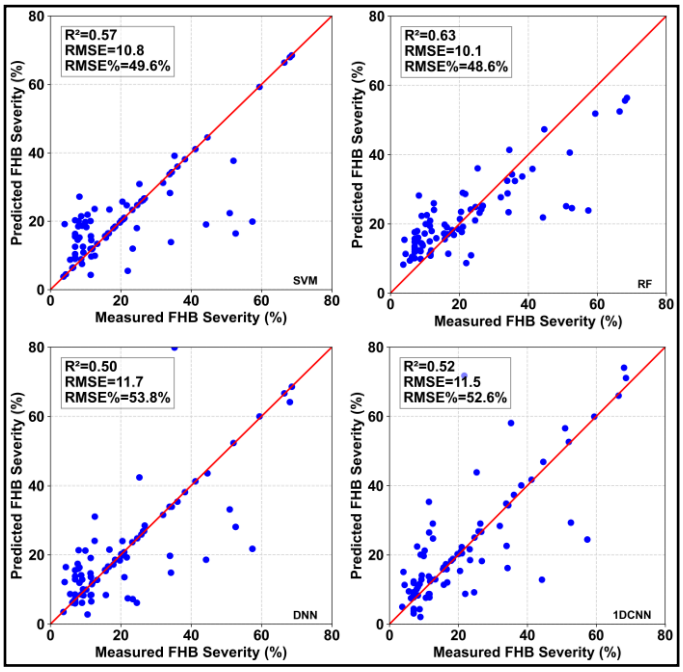

Fig. 7. Measured vs. Predicted FHB Disease Severity (%) comparison when using combined spectral and texture features

V. CONCLUSIONS

This study examines the potential of integrating UAS remote sensing with conventional machine learning and deep learning models for predicting wheat FHB disease severity through classification and regression approaches. Our results show that UAS multispectral imagery-derived spectral, textural, and combined spectral-textural features are important variables for predicting FHB disease severity. Additionally, coupled UAS remote sensing with machine and deep learning-based modeling is an effective approach for wheat FHB disease severity estimation and assessment. It is important to note that UAS remote sensing and machine learning-based estimation of wheat FHB disease still face challenges. These challenges are primarily due to the relatively small sample size available for training models, and the limited contribution of FHB-affected wheat spikes to the overall canopy signals captured by UAS imagery at the plot level. Future work could focus on further evaluating the potential of deep learning models by obtaining larger training samples or by employing pre-trained models through a transfer learning approach. Additionally, acquiring higher-resolution UAS imagery (e.g., at the millimeter level) and deriving spectral and texture features specifically from wheat spike pixels (excluding those of wheat leaves) could lead to improved FHB prediction results.

ACKNOWLEDGMENT

This work was supported partially by South Dakota State University (SDSU) RSCA fund (#334709), SDSU Agricultural Experiment Station and USDA-NIFA Hatch Projects (#SD00H757), USDA-NIFA Wheat CAP project (2022-68013-36439), and South Dakota Wheat Commission.

References

[1] J. Tack, A. Barkley, and L. L. Nalley, "Effect of warming temperatures on US wheat yields," *Proceedings of the National Academy of Sciences*, vol. 112, no. 22, pp. 6931-6936, 2015.

[2] N. Senapati *et al.*, "Global wheat production could benefit from closing the genetic yield gap," *Nature Food*, vol. 3, no. 7, pp. 532-541, 2022.

[3] E. C. Rojas *et al.*, "Fusarium head blight modifies fungal endophytic communities during infection of wheat spikes," *Microbial ecology*, vol. 79, no. 2, pp. 397-408, 2020.

[4] C. Dweba *et al.*, "Fusarium head blight of wheat: Pathogenesis and control strategies," *Crop protection*, vol. 91, pp. 114-122, 2017.

[5] H. Linsheng, Z. Qing, Z. Dongyan, L. Fenfang, X. Chao, and Z. Jinling, "Early diagnosis of wheat powdery mildew based on Relief-F band screening, vol. 47, no. 5, pp. 523001-0523001 (8), 2018.

[6] E. Bauriegel and W. B. Herppich, "Hyperspectral and chlorophyll fluorescence imaging for early detection of plant diseases, with special reference to Fusarium spec. infections on wheat," *Agriculture*, vol. 4, no. 1, pp. 32-57, 2014.

[7] J. Zhang *et al.*, "Monitoring plant diseases and pests through remote sensing technology: A review," *Computers and Electronics in Agriculture*, vol. 165, p. 104943, 2019.

[8] L. Liu, Y. Dong, W. Huang, X. Du, and H. Ma, "Monitoring wheat fusarium head blight using unmanned aerial vehicle hyperspectral imagery," *Remote Sensing*, vol. 12, no. 22, p. 3811, 2020.

[9] H. Tao *et al.*, "Estimation of crop growth parameters using UAV-based hyperspectral remote sensing data," *Sensors*, vol. 20, no. 5, p. 1296, 2020.

[10] H. Ye *et al.*, "Recognition of banana fusarium wilt based on UAV remote sensing," *Remote Sensing*, vol. 12, no. 6, p. 938, 2020.

[11] G. Mustafa *et al.*, "Enhancing fusarium head blight detection in wheat crops using hyperspectral indices and machine learning classifiers," *Computers and Electronics in Agriculture*, vol. 218, p. 108663, 2024.

[12] Q. Hong *et al.*, "A lightweight model for wheat ear fusarium head blight detection based on RGB images," *Remote Sensing*, vol. 14, no. 14, p. 3481, 2022.

[13] Y. Xiao, Y. Dong, W. Huang, L. Liu, and H. Ma, "Wheat fusarium head blight detection using UAV-based spectral and texture features in optimal window size," *Remote Sensing*, vol. 13, no. 13, p. 2437, 2021.

[14] C. Gao *et al.*, "Monitoring of wheat Fusarium head blight on spectral and textural analysis of UAV multispectral imagery," *Agriculture*, vol. 13, no. 2, p. 293, 2023.

[15] H. Zhang *et al.*, "Detection of wheat Fusarium head blight using UAV-based spectral and image feature fusion," *Frontiers in plant science*, vol. 13, p. 1004427, 2022.

[16] D.-Y. Zhang *et al.*, "Integrating spectral and image data to detect Fusarium head blight of wheat," *Computers and Electronics in Agriculture*, vol. 175, p. 105588, 2020.

[17] D. Todey, J. Trobec, and H. M. Mogil, "South Dakota's Climate and Weather," *Weatherwise: THE POWER, THE BEAUTY, THE EXCITEMENT*, vol. 62, no. 6, pp. 16-23, 2009.

[18] J. Rouse Jr, R. H. Haas, D. Deering, J. Schell, and J. C. Harlan, "Monitoring the vernal advancement and retrogradation (green wave effect) of natural vegetation," 1974.

[19] G. Rondeaux, M. Steven, and F. Baret, "Optimization of soil-adjusted vegetation indices," *Remote sensing of environment*, vol. 55, no. 2, pp. 95-107, 1996.

[20] R. M. Haralick, K. Shanmugam, and I. H. Dinstein, "Textural features for image classification," *IEEE Transactions on systems, man, and cybernetics*, no. 6, pp. 610-621, 1973.

[21] M. Maimaitijiang, V. Sagan, P. Sidike, S. Hartling, F. Esposito, and F. B. Fritschi, "Soybean yield prediction from UAV using multimodal data fusion and deep learning," *Remote sensing of environment*, vol. 237, p. 111599, 2020.

[22] S. Hartling, V. Sagan, P. Sidike, M. Maimaitijiang, and J. Carron, "Urban tree species classification using a WorldView-2/3 and LiDAR data fusion approach and deep learning," *Sensors*, vol. 19, no. 6, p. 1284, 2019.

[23] I. Goodfellow, *Deep Learning*. MIT Press, 2016.